The Journal of Neuroscience, October 15, 2001, 21(20):8015–8025

Induction of Mossy Fiber→CA3 Long-Term Potentiation Requires Translocation of Synaptically Released Zn^{2+}

Yang Li,[1] Christopher J. Hough,[2] Christopher J. Frederickson,[3,4] and John M. Sarvey[1]

Departments of [1]Pharmacology and [2]Psychiatry, Uniformed Services University of the Health Sciences, Bethesda, Maryland 20814, and [3]NeuroBioTex, Inc. and [4]Departments of Biomedical Engineering and Anatomy and Neuroscience, The University of Texas Medical Branch, Galveston, Texas 77550

The mammalian CNS contains an abundance of chelatable Zn^{2+} sequestered in the vesicles of glutamatergic terminals. These vesicles are particularly numerous in hippocampal mossy fiber synapses of the hilar and CA3 regions. Our recent observation of frequency-dependent Zn^{2+} release from mossy fiber synaptic terminals and subsequent entry into postsynaptic neurons has prompted us to investigate the role of synaptically released Zn^{2+} in the induction of long-term potentiation (LTP) in field CA3 of the hippocampus. The rapid removal of synaptically released Zn^{2+} with the membrane-impermeable Zn^{2+} chelator CaEDTA (10 mM) blocked induction of NMDA receptor-independent mossy fiber LTP by high-frequency electrical stimulation (HFS) in rat hippocampal slices. Mimicking Zn^{2+} release by bath application of Zn^{2+} (50–100 μM) without HFS induced a long-lasting potentiation of synaptic transmission that lasted more than 3 hr. Moreover, our experiments indicate the effects of Zn^{2+} were not attributable to its interaction with extracellular membrane proteins but required its entry into presynaptic or postsynaptic neurons. Co-released glutamate is also essential for induction of LTP under physiological conditions, in part because it allows Zn^{2+} entry into postsynaptic neurons. These results indicate that synaptically released Zn^{2+}, acting as a second messenger, is necessary for the induction of LTP at mossy fiber→CA3 synapses of hippocampus.

Key words: zinc; long-term potentiation; CA3; hippocampus; CaEDTA; mossy fiber; plasticity; Na-pyrithione; Newport Green; synaptic transmission

The mammalian CNS contains an abundance of chelatable Zn^{2+} sequestered in the vesicles of glutamatergic terminals. These vesicles are particularly numerous in hippocampal mossy fiber synapses of the hilar and CA3 regions (Haug, 1967; Perez-Clausell and Danscher, 1985; Frederickson, 1989; Frederickson et al., 2000; Li et al., 2001). A possible synaptic signaling role for Zn^{2+} is suggested by its interactions with excitatory and inhibitory amino acid receptors such as NMDA, AMPA, and GABA receptors (Peters et al., 1987; Westbrook and Mayer, 1987). Zn^{2+} accumulates in synaptic vesicles through a specific Zn^{2+} transporter, termed Zn transporter 3 (Palmiter et al., 1996). Vesicular Zn^{2+} release can be elicited by electrical stimulation (Howell et al., 1984; Li et al., 2001) or membrane depolarization (by elevating extracellular K^+ concentration; Assaf and Chung, 1984; Anisksztejn et al., 1987; Li et al., 2001). Characterization of this Zn^{2+} release has revealed that it is released in the same manner as neurotransmitters: the release is Ca^{2+}-dependent and tetrodotoxin-sensitive (Li et al., 2001). Recently, it has been shown that extracellular Zn^{2+} enters neurons through glutamate receptors and voltage-dependent Ca^{2+} channels (VDCCs; Weiss and Sensi, 2000). Despite a considerable amount of evidence suggesting that Zn^{2+} acts in concert with neurotransmitters in the CNS, a specific physiological role for synaptically released Zn^{2+} has yet to be identified.

In addition to having routes of entry into neurons that are activated during nerve transmission, Zn^{2+} is known to interact with the protein kinases and phosphatases of signal transduction pathways that affect changes in gene expression (Brewer et al., 1979; Hubbard et al., 1991; Weinberger and Rostas, 1991; Quest et al., 1992; Maret et al., 1999; Park and Koh, 1999; Lengyel et al., 2000). Our recent observation (Li et al., 2001) of frequency-dependent Zn^{2+} release from mossy fiber synaptic terminals and subsequent entry into postsynaptic neurons of the dentate gyrus has suggested to us that Zn^{2+} might play a role in the normal physiological function of these neurons. Detectable Zn^{2+} release varied over a range of frequencies (10–200 Hz), which included frequencies used to induce long-term potentiation (LTP). We hypothesized that translocation of Zn^{2+} across synapses might be an important physiological signal mediating some aspects of synaptic plasticity, such as LTP.

LTP is an important model for studying the cellular mechanisms of neuronal plasticity, learning, and memory. Zn^{2+}-deficient rats and rhesus monkeys experience a learning and working memory deficit (Golub et al., 1995). Although the possibility that Zn^{2+} released from the mossy fiber bouton might be involved in hippocampal LTP has been proposed by Weiss et al (1989) more than a decade ago, much is still unknown about the involvement of synaptically released Zn^{2+} in synaptic plasticity. Recently, two groups failed to alter the induction of mossy fiber LTP by removing synaptically released Zn^{2+} with the Zn^{2+} chelator CaEDTA (Lu et al., 2000; Vogt et al., 2000). Using

Received May 7, 2001; revised July 20, 2001; accepted July 23, 2001.

This research was supported by grants from the Brain Injury Association and National Institutes of Health Grant NS23865 to J.M.S., generous support from Theodore and Vada Stanley to C.J.H., and in part by National Institutes of Health Grants NS40215 and NS38585 to C.J.F. We thank Richard Thompson for helpful discussions and Ajay Verma for assistance with measurement of free Ca^{2+}.

The opinions and assertions contained herein are the private opinions of the authors and are not to be construed as official or reflecting the views of the Uniformed Services University of the Health Sciences or the United States Department of Defense.

Correspondence should be addressed to John Sarvey, Department of Pharmacology, Uniformed Services University of the Health Sciences, 4301 Jones Bridge Road, Bethesda, MD 20814. E-mail: jsarvey@usuhs.mil.

fluorescence imaging, we show here that although a low concentration (1 mM) of CaEDTA was not sufficient to prevent synaptically released Zn^{2+} from reaching postsynaptic neurons after high-frequency stimulation (HFS), a higher concentration (10 mM) of Zn^{2+} chelator was. This treatment blocked the induction of LTP. Moreover, perfusion of slices with exogenous Zn^{2+} (50–100 μM) could also induce long-lasting potentiation of the EPSP in the absence of HFS. Finally, our experiments indicate that the effects of Zn^{2+} were not attributable to its interaction with extracellular membrane proteins but required its entry into presynaptic or postsynaptic neurons.

MATERIALS AND METHODS

Hippocampal slice preparation. Experiments were conducted according to the principles set forth in the *Guide for Care and Use of Laboratory Animals* (Institute of Animal Resources, National Research Council, National Institutes of Health publication 74-23). Male adult Sprague Dawley rats were anesthetized with ketamine hydrochloride and decapitated. The brain was quickly removed and immersed in ice-cold (1–4°C) artificial CSF (ACSF) with the composition of (in mM): NaCl, 124; KCl, 1.75; $MgSO_4$, 1.3; $CaCl_2$, 2.4; KH_2PO_4, 1.25; $NaHCO_3$, 26; and dextrose, 10, continuously bubbled with 95% O_2 and 5% CO_2. Transverse hippocampal slices 400 μm in thickness were prepared using a McIlwain tissue chopper (Brinkmann Instruments, Westbury, NY) or Vibratome (Frederic Haer, Brunswick, ME). Slices were incubated in a 95% O_2-5% CO_2-saturated interface recording chamber for at least 1 hr before recording at 32°C.

Electrical stimulation and recordings. The mossy fiber→CA3 pyramidal neuron responses were induced by the stimulation of mossy fiber axons with a 100-μm-diameter monopolar Teflon-insulated stainless steel wire electrode, exposed only at the tip (Fig. 1*A*). Extracellular recordings were obtained using glass micropipettes filled with 2 M NaCl, 2–6 MΩ resistance. The recording electrodes were placed at least 500 μm from the stimulating electrodes along the trajectory of the mossy fiber pathway. The recording electrodes were lowered to a distance of 80–100 μm beneath the slice surface. Paired pulse facilitation of the EPSP was conducted at 20 and 80 msec interpulse intervals. Slices were accepted for further study when the mossy fiber pathway showed facilitation at the 80 msec interval. Because of the complex circuitry of area CA3, the metabotropic Glu receptor (mGluR) II agonist 2-(2,3-dicarboxycyclopropyl)glycine (DCG-IV) was used at the end of the experiments to verify that the signal was generated by mossy fiber inputs (Kamiya et al., 1996). D-APV (50 μM) was added in ACSF to prevent contamination with the NMDA receptor-dependent pathway converging on CA3 neurons. For inducing mossy fiber→CA3 LTP, test stimuli were delivered to mossy fiber axons every 30 sec (0.03 Hz). The stimulus intensity was set to produce ~30% of the maximum EPSP. HFS consisted of one train of 100 Hz lasting 2 sec at the intensity that induced the maximum EPSP. The maximal negative initial slope of the mossy fiber→CA3 EPSP was calculated and normalized to 30 min baseline value (defined as 100%).

Zn^{2+} imaging. Methods for imaging Zn^{2+} fluorescence have been published (Li et al., 2001). For extracellular Zn^{2+} fluorescence imaging, hippocampal slices were preloaded with 20 μM Newport Green (Molecular Probes, Eugene, OR) dipotassium salt at room temperature in the dark for at least 30 min. For intracellular Zn^{2+} imaging, the slices were preloaded with 50 μM diacetate ester of Newport Green in 0.5% dimethylsulfoxide containing 0.1% pluronic acid for 1 hr and then washed with ACSF. The Zn^{2+}-selective fluorescent dye Newport Green has a K_d of 1 μM for Zn^{2+}. Newport Green fluorescence was minimally affected by the presence of Ca^{2+} and Mg^{2+} at physiological concentrations (Li et al., 2001). Ca^{2+} or Mg^{2+} (up to 10 mM), in the absence of Zn^{2+}, had little effect on the dye fluorescence emission. All experiments were performed at 32°C under constant ACSF perfusion on the thermostatically heated stage of an inverted microscope (Axiovert 140; Zeiss, Oberkochen, Germany) coupled to a Delta Ram xenon light source (PTI, Manmouth Junction, NJ) and monochromator set to 506 nM. Emitted light images at 533 nm or greater were acquired at rates of 2–30 Hz through a 10× 0.1 numerical aperture objective with an intensified CCD camera (PTI IC-100) and digitized using ImageMaster software (PTI). Autofluorescence was below the detection limits of the camera, and photobleaching was negligible under these conditions; neither was subtracted from the data. Images in Figures 7 and 8 were captured by an Orca digital camera (Hamamatsu, Hamamatsu City, Japan) using Open Lab Software (Improvision). To induce the release of Zn^{2+} from mossy fiber terminals, bipolar electrodes 300–500 μm apart were used for electrical stimulation to excite mossy fiber axons. Trains of orthodromic stimuli (100 Hz, 200 μsec pulses at 500 μA unless otherwise noted) of various frequencies were delivered using an S44 stimulator and a PS1U6 photoelectric stimulus isolation unit (Grass Electronics, Quincy, MA).

RESULTS

Rapid chelation of synaptically released Zn^{2+} blocks induction of mossy fiber LTP

To determine whether Zn^{2+} is involved in this specific form of synaptic plasticity, we examined the effects of applying CaEDTA, a cell-impermeable extracellular Zn^{2+} chelator ($K_d = 10^{-16.4}$ M) that does not appreciably alter Ca^{2+} concentration (Fredens and Danscher, 1973; Dawson et al., 1986; Bers et al., 1994). Stimulation of the mossy fiber axons produced an extracellular field EPSP recorded in the dendritic region (stratum lucidum) of pyramidal neurons in field CA3 of hippocampal slices (Fig. 1*A*). In control slices, brief HFS produced EPSP potentiation (mossy fiber LTP; Fig. 1*B*). The averaged normalized EPSP slope 30 min after HFS was 193 ± 10% (mean ± SEM; $n = 9$) of baseline, and the potentiation was stable for >3 hr (maximum recording duration) after our standard recording procedure (Bramham and Sarvey, 1996). To chelate Zn^{2+} released by HFS and to prevent it from reaching postsynaptic neurons, we perfused slices with 10 mM CaEDTA for 10 min before and 10 min after HFS. This treatment blocked induction of LTP (103 ± 4%, mean ± SEM; $n = 11$; Fig. 1*C*). Although there was an initial small post-tetanic potentiation immediately after HFS, it decayed to baseline within 5–10 min. These results suggest that Zn^{2+} released during HFS plays an essential role in the induction of mossy fiber LTP. To determine whether chelation of Zn^{2+} could alter the maintenance of LTP, CaEDTA was applied 10 min after HFS. Figure 1*D* shows that CaEDTA (10 mM) had no effect on established LTP, suggesting that the removal of Zn^{2+} after HFS did not influence the late, or maintenance, phase of LTP.

Kinetics of Zn^{2+} chelation by CaEDTA

To verify that Zn^{2+} released from mossy fiber terminals by HFS was adequately chelated by 10 mM CaEDTA, we loaded slices with the selective extracellular Zn^{2+} fluorescent indicator Newport Green dipotassium salt (cell-impermeable; Molecular Probes) and visualized Zn^{2+} release after stimulation in the presence and absence of CaEDTA. In a previous study (Li et al., 2001), we found that electrically stimulated Zn^{2+} release was frequency-dependent and could be detected with as little as 10 Hz stimulation at 500 μA. The degree of Zn^{2+} release also increased with increasing stimulus amplitudes ranging from 20 to -500 μA (100 Hz over 5 sec). Ten millimolar CaEDTA chelated 85% of the synaptically released Zn^{2+}, as indicated by Newport Green fluorescence (Fig. 2*A*). This result verifies that the effect of CaEDTA on LTP induction in mossy fiber→CA3 synapses was achieved by its selective chelation of the synaptically released Zn^{2+} from mossy fiber terminals. After bath perfusion of 10 mM CaEDTA for 10 min, followed by washout of the CaEDTA, we could still induce normal release of Zn^{2+} in normal ACSF (data not shown). On the other hand, a lower concentration of CaEDTA (1 mM) failed to reduce the extracellular Zn^{2+} after HFS, as evidenced by its inability to reduce Newport Green fluorescence (Fig. 2*A*). Therefore, induction of LTP was essentially unaffected in 1 mM CaEDTA (Fig. 2*B*).

These results are consistent with our calculations of the kinetics of Zn^{2+} chelation in ACSF containing CaEDTA. Our calcula-

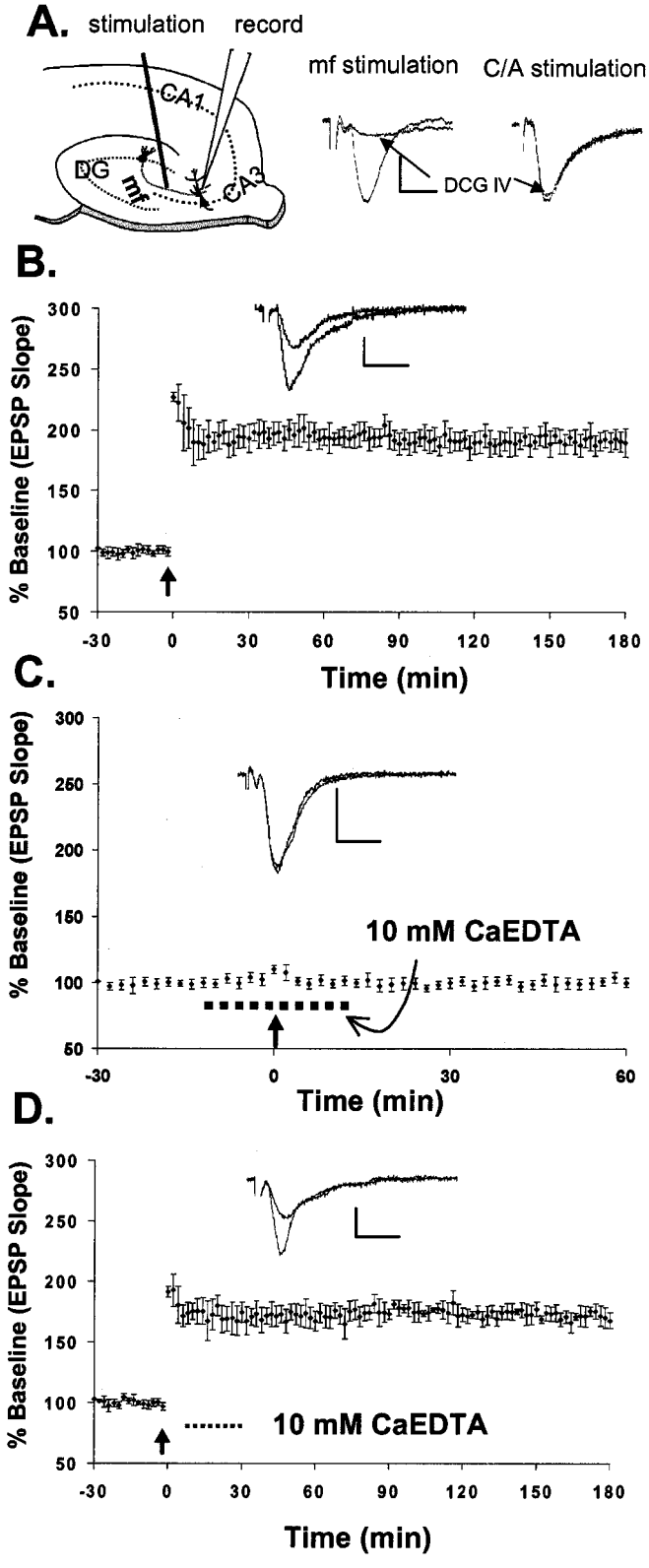

Figure 1. Rapid chelation of extracellular Zn^{2+} blocks induction of mossy fiber LTP. *A*, Schematic of a hippocampal slice showing stimulating and recording sites. The *traces* on the *right* show the field EPSPs evoked by stimulation of mossy fibers (*mf*) and the commissural–associational pathway. The group II mGluR agonist DCG-IV (5 μM) selectively blocked mossy fiber responses to 17.3 ± 2% ($n = 6$) of those before drug application but had little effect on the responses (to 97.7 ± 1.9%; $n = 6$) evoked by stimulating the commissural–associational fibers in the stratum radiatum (electrode not shown). *B*, Mossy fiber LTP (193 ± 10%; $n = 9$) induced by HFS after recording a 30 min baseline (see Materials and Methods). *C*, HFS failed to induce mossy fiber LTP (103 ± 4%; $n = 11$) in the presence of 10 mM CaEDTA (*dashed line*). *D*, Adding CaEDTA (10 mM; *dashed line*) 10 min after induction of LTP did not affect the late, or maintenance, phase of LTP (175 ± 8%; $n = 3$). Each *point* in *B–D* represents the averaged and normalized EPSP initial negative slope, and error bars indicate SEM. *Arrows* indicate HFS (100 Hz, 2 sec). *B–D, Insets*, EPSP recorded during baseline and at the end of the recording period after HFS. Calibration: 1.0 mV, 5 msec.

tions predict that, in 10 mM CaEDTA, 100 μM extracellular Zn^{2+} would be reduced to 33 nM within 0.1 msec, whereas in 1 mM CaEDTA, this concentration of Zn^{2+} would only be reduced to 15 μM in 0.1 msec (Fig. 3; and Appendix). Thus, we suggest that 10 mM CaEDTA effectively removes Zn^{2+} released from nerve terminals by HFS before its physiological function can be performed (Basolo and Pearson, 1967; Davis et al., 1999). This explains why 1 mM CaEDTA failed to block induction of LTP in this study (Fig. 2*B*) and in previous studies (Lu et al., 2000; Vogt et al., 2000).

Removal of synaptically released Zn^{2+} does not affect basal synaptic transmission

Disodium EDTA nominally saturated with equimolar Ca^{2+} (CaEDTA) has been used to add the chelator to physiological buffers such as ACSF without appreciably reducing the concentration of extracellular Ca^{2+}, which is essential for normal synaptic transmission. To verify this, we measured the concentration of free Ca^{2+} in ACSF using a Ca^{2+} electrode. Addition of 1 mM CaEDTA did not alter the free Ca^{2+}. Addition of 10 mM CaEDTA reduced the measured concentration of free Ca^{2+} from 2.25 ± 0.02 mM (mean ± SEM; $n = 3$) to 2.03 ± 0.03 mM (mean ± SEM; $n = 3$; Fig. 4*A*). This was probably attributable to incomplete saturation of the EDTA with Ca^{2+} during its manufacture. When we added an extra 0.22 mM $CaCl_2$ to ACSF containing 10 mM CaEDTA to compensate for the Ca^{2+} deficit, the concentration of free Ca^{2+} was 2.25 ± 0.01 mM (mean ± SEM; $n = 3$).

Ten millimolar CaEDTA had no effect on basal synaptic transmission elicited by low-frequency stimulation, as measured by the initial slope of the EPSP at mossy fiber→CA3 synapses (Fig. 4*B*). The chelator at this concentration also had no effect on paired pulse facilitation, a physiological property of presynaptic terminal function at mossy fiber→CA3 synapses (Fig. 4*C*). Our data demonstrate that basal synaptic function is not altered in the presence of 10 mM Zn^{2+} chelator. Thus, the data suggest that the effects of CaEDTA we observed were attributable to changes in Zn^{2+} concentration.

Mimicking Zn^{2+} release by adding exogenous Zn^{2+} induces a long-lasting potentiation of synaptic transmission

In the experiments described above, 10 mM CaEDTA apparently blocked the induction of LTP, because it chelated the Zn^{2+} released during HFS. We then hypothesized that the addition of exogenous Zn^{2+} to extracellular bathing solution in the absence of HFS would enhance the strength of synaptic transmission and would induce a long-lasting potentiation of the EPSP in field CA3. As shown in Figure 5*A*, the EPSP was gradually potentiated to 195 ± 17% of baseline (mean ± SEM; $n = 8$) during a 20 min exposure to 100 μM Zn^{2+} and remained potentiated for >3 hr. Zn^{2+} does not affect the afferent volley in our experimental

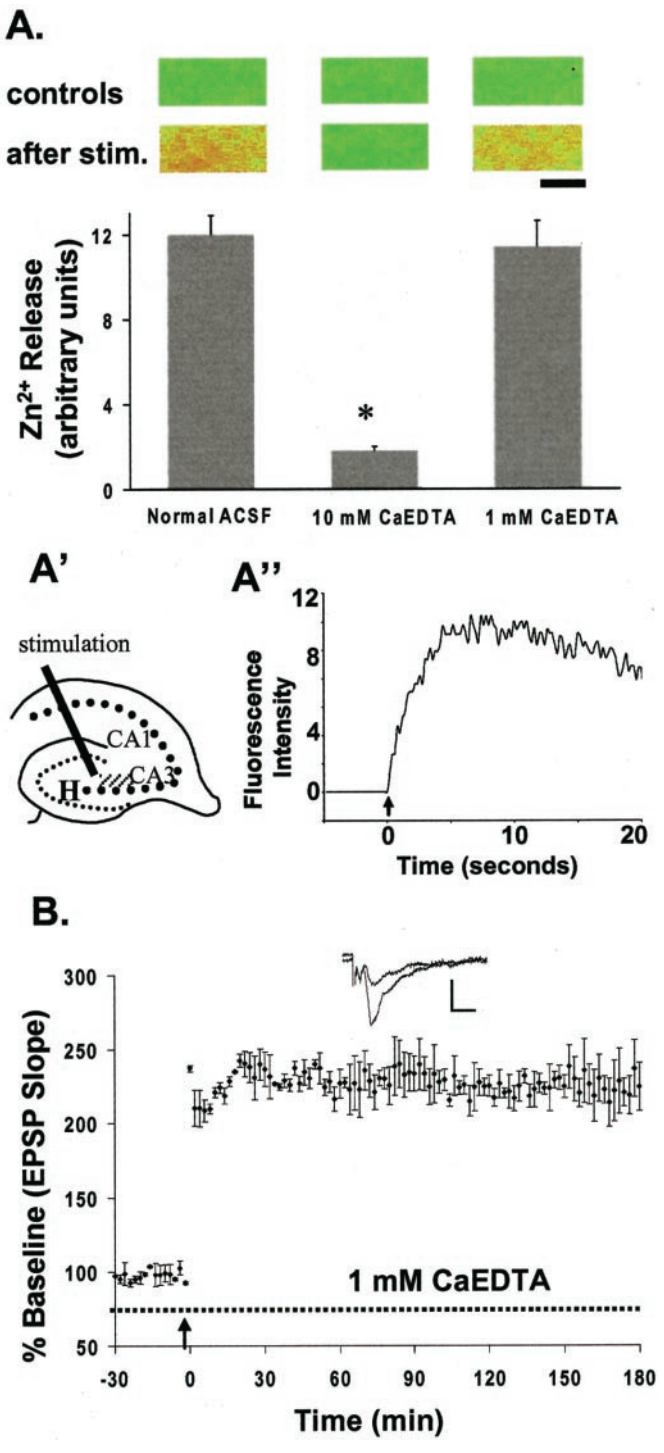

Figure 2. Zn^{2+} release with electrical stimulation and the effects of Zn^{2+} chelator. *A*, Extracellular Zn^{2+} released from terminals after electrical stimulation (*stim.*) was measured as the peak emission intensity of extracellular Newport Green fluorescence in the absence and presence of Zn^{2+} chelator (3 determinations; error bars indicate SE). The paired images on *top* correspond with each condition of the *bar graph*. They were acquired before (controls in the *first row*) and after (*second row*) HFS (200 μsec, 0.5 mA pulses for 5 sec). In these false-color images, increasing intensity of Zn^{2+} fluorescence is represented by the spectrum ranging from *blue* (the lowest) to *red* (the highest). Scale bar, 100 μm. *A'*, The *hatched area* represents the region where images were acquired. *H*, Hilus. Values plotted are the mean ± SEM; $n = 4$; $^*p < 0.05$. *A"*, Plot of electrical stimulation (100 Hz for 5 sec)-evoked rapid release of Zn^{2+} from neuronal terminals measured by changes in Newport Green fluorescence intensity (arbitrary units). The *arrow* indicates the beginning of stimulation. *B*, A low concentration of CaEDTA (1 mM; *dashed line*) had little effect on mossy fiber LTP (227 ± 11%; $n = 4$) evoked by HFS. Each *point* is the averaged and normalized EPSP initial negative slope, and error bars indicate SEM. *Arrows* indicate the time giving HFS (100 Hz, 2 sec). Calibration: 1.0 mV, 5 msec.

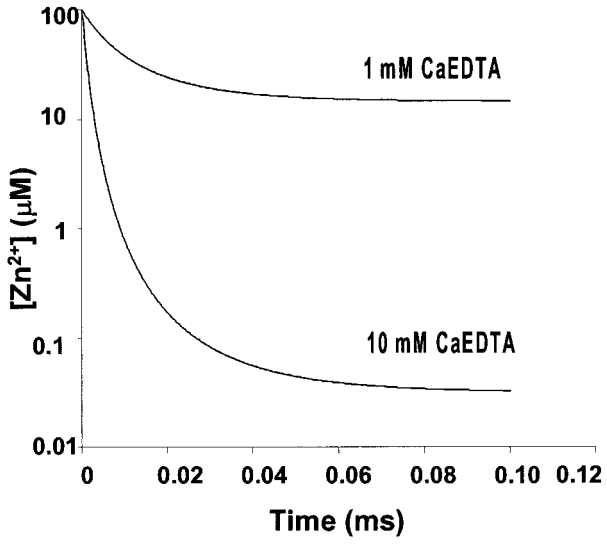

Figure 3. Calculated kinetics of chelation of 100 μM Zn^{2+} in ACSF by 1 and 10 mM CaEDTA. The rate of chelation of 100 μM Zn^{2+} by 1 and 10 mM CaEDTA was estimated using published and estimated forward and reverse rate constants as described in Appendix. Only the first 0.1 msec after the release of Zn^{2+} is given. Equilibrium conditions are assumed for 1 and 10 mM CaEDTA in ACSF in the absence of Zn^{2+} at time 0. Note that, under these conditions, equilibrium concentrations after introduction of 100 μM Zn^{2+} are not achieved within this time frame.

conditions. Throughout this experiment, the only stimulation applied was low-frequency test stimuli. These data strongly suggest that Zn^{2+} is able to enhance synaptic strength at mossy fiber→CA3 synapses. Once long-lasting potentiation of the EPSP was established, washing away the exogenous Zn^{2+} with ACSF containing 10 mM CaEDTA (10 min) did not halt the potentiation (Fig. 5*A*). This result also indicates that the potentiating effect of Zn^{2+} was not attributable to its prolonged binding to plasma membrane components. Figure 5*B* shows the frequency (given as a percentage) with which various concentrations of Zn^{2+} induced long-lasting potentiation. In these concentration–response studies, we could reliably induce long-lasting potentiation of the EPSP in concentrations of 50 μM (71%; $n = 7$) and 100 μM (100%; $n = 9$) Zn^{2+}. Estimates of the concentration of Zn^{2+} released from the mossy fibers during HFS have ranged from 10 to 100 μM (Vogt et al., 2000; Li et al., 2001); Zn^{2+} concentration could reach as much as 300 μM under extreme conditions (Frederickson, 1989). In the presence of 300 μM Zn^{2+}, we observed long-lasting potentiation of the EPSP in less than half the slices tested ($n = 7$; Fig. 5*B*). This high failure rate might be caused by the neurotoxic effect of Zn^{2+} at this high concentration (Frederickson et al., 2000).

Glutamate facilitates the potentiating effect of Zn^{2+}

Because glutamate is also released from mossy fiber terminals during electrical stimulation, it is reasonable to expect that, under physiological conditions, both glutamate and Zn^{2+} are required

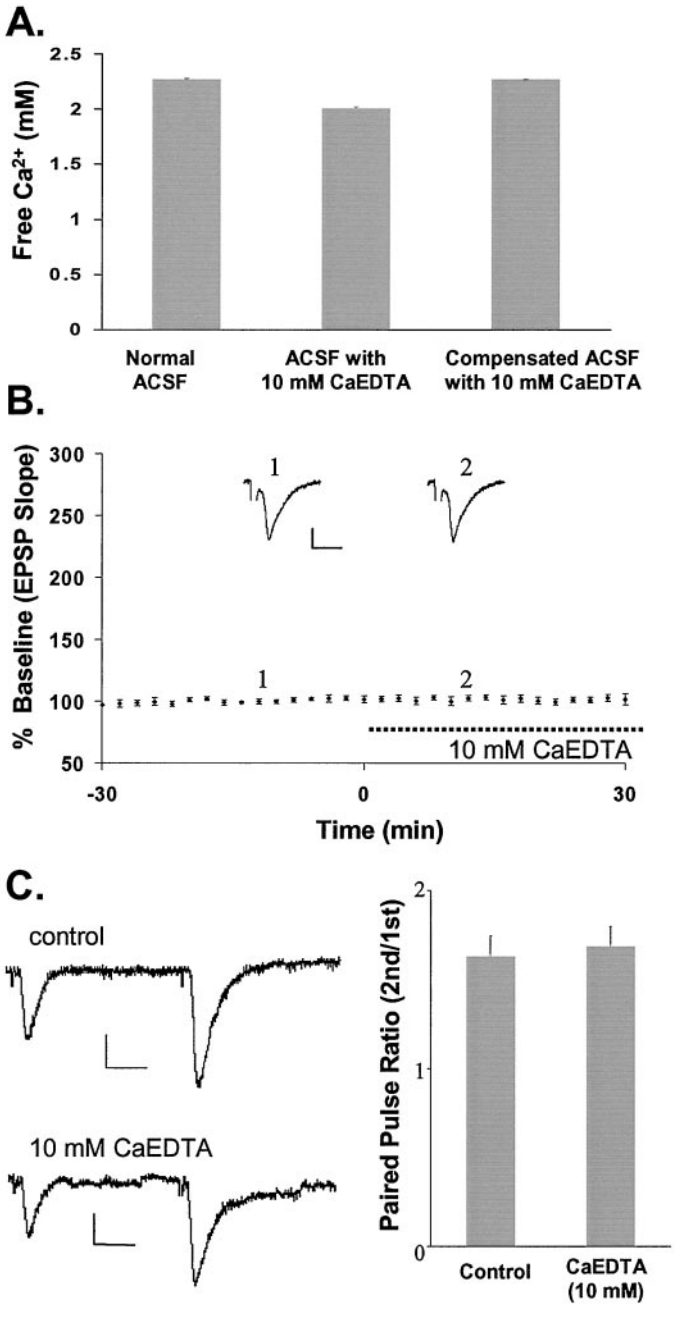

Figure 4. Exposure of slices to a high concentration of CaEDTA does not alter normal basal synaptic responses at mossy fiber→CA3 synapses with low-frequency stimulation. *A*, Free Ca^{2+} was measured in normal ACSF (*left bar*) and in ACSF containing 10 mM CaEDTA (*middle bar*). The *right bar* shows the concentration of Ca^{2+} measured in ACSF containing 10 mM CaEDTA with an additional 0.22 mM $CaCl_2$ (2.4 mM $CaCl_2$ in normal ACSF) added to restore free Ca^{2+} to the level in normal ACSF. *B*, Plot of the EPSP against time, with bath-applied CaEDTA (10 mM) indicated by a *dashed line*. Each *point* represents the averaged initial slope of evoked EPSP ($n = 6$). The averaged values were then normalized to the mean initial slope during 30 min baseline recording (percent ± SEM). The *traces* on *top* represent recording before (*1*) and during (*2*) CaEDTA perfusion. *C*, The paired pulse ratio is unaffected by the addition of CaEDTA, as shown on the *left*. The *bar graph* demonstrates the average paired pulse ratios from six recordings in which two stimuli were given 40 msec apart in the presence and absence of CaEDTA. Calibration in *B, C*: 0.5 mV, 5 msec.

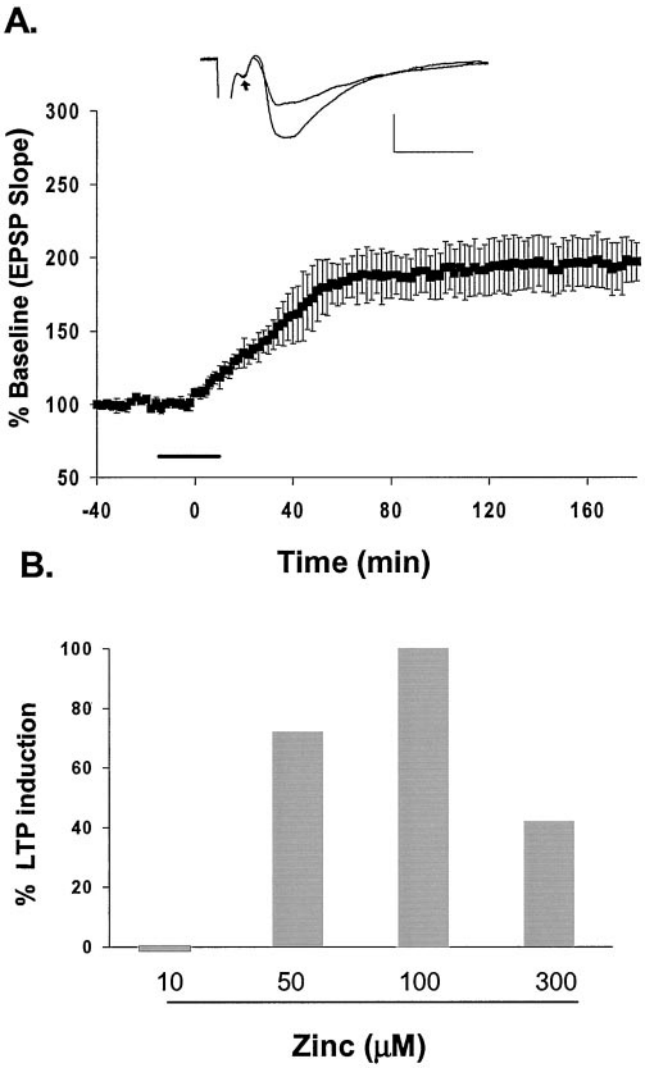

Figure 5. Exogenous Zn^{2+} induces long-lasting potentiation of the EPSP. *A*, Plot of exogenous Zn^{2+}-induced long-lasting potentiation. Zn^{2+} (100 μM) was applied for 20 min (*line*) after recording a 30 min baseline. Application of Zn^{2+} was followed by wash with 10 mM CaEDTA. *Inset*, EPSP recorded before and after exposure to Zn^{2+}. Note that the afferent volley (*arrow*) was not affected. *B*, Percentage of LTP induced by different concentrations of exogenous Zn^{2+}. Calibration in *A*: 1.0 mV, 5 msec.

for LTP induction in these terminals. In our next set of experiments, we sought to verify that simultaneous application of exogenous glutamate and Zn^{2+} together is sufficient to induce long-lasting potentiation. In these experiments, co-perfusion of glutamate and Zn^{2+}, to imitate the co-release of both from synaptic terminals, induced long-lasting potentiation (Fig. 6*A*) similar to that induced by Zn^{2+} alone (Fig. 5*A*). The mean potentiated EPSP slope was 241 ± 11% (mean ± SEM; $n = 6$) of baseline, and the potentiation was stable for >3 hr. Glutamate alone, however, in the presence of 10 mM CaEDTA induced only a transient EPSP potentiation, followed by an immediate return to baseline after glutamate washout (Fig. 6*A*). This result implies that glutamate itself could not induce a persistent EPSP potentiation. As summarized in Figure 6*B*, the effect of Zn^{2+} on induction of long-lasting potentiation was modulated by the level of glutamate in the bath. With the standard low-frequency (0.03 Hz) test stimulation, adding both glutamate and Zn^{2+} caused a more

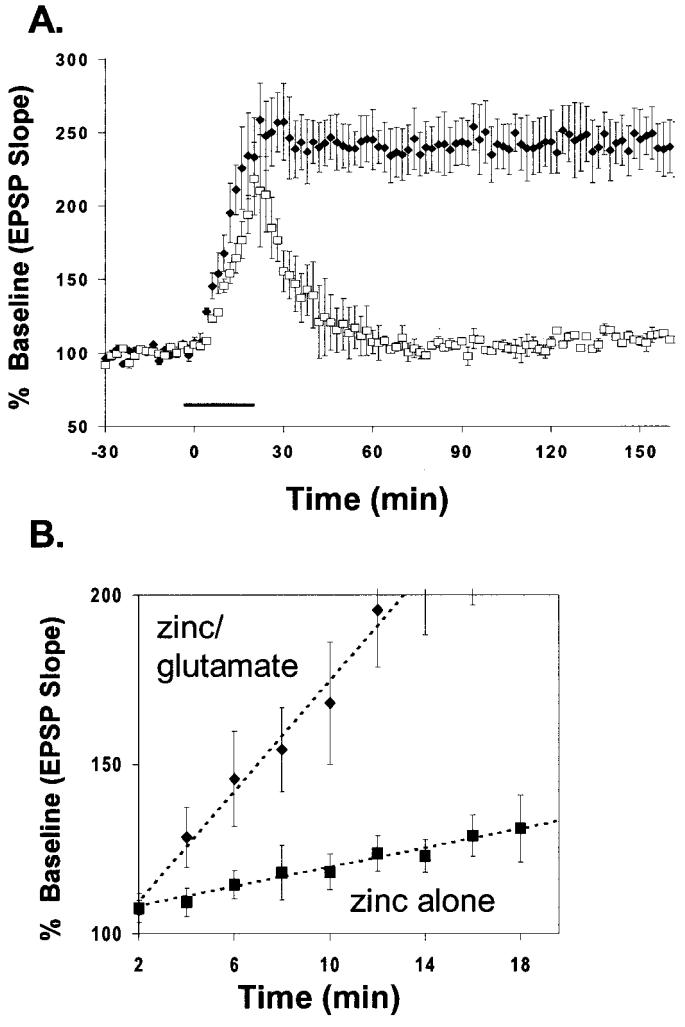

Figure 6. Glutamate facilitates the potentiating effect of Zn^{2+}. *A*, Co-application of glutamate (100 μM) and Zn^{2+} (100 μM) expeditiously potentiated EPSPs; potentiation lasted several hours (*filled diamonds*). Glutamate alone (*open squares*; in the presence of CaEDTA) failed to induce long-lasting potentiation of the EPSP. Exogenous glutamate and Zn^{2+} were applied for 20 min (*line*) after recording a 30 min baseline. Application of glutamate or Zn^{2+} with glutamate was followed by wash with 10 mM CaEDTA. *B*, Comparison of the rate of onset of long-lasting potentiation induced by Zn^{2+} alone and Zn^{2+} plus glutamate. Each *point* represents the averaged, normalized EPSP initial slope ± SEM from data in Figure 5*A* and *A*, respectively.

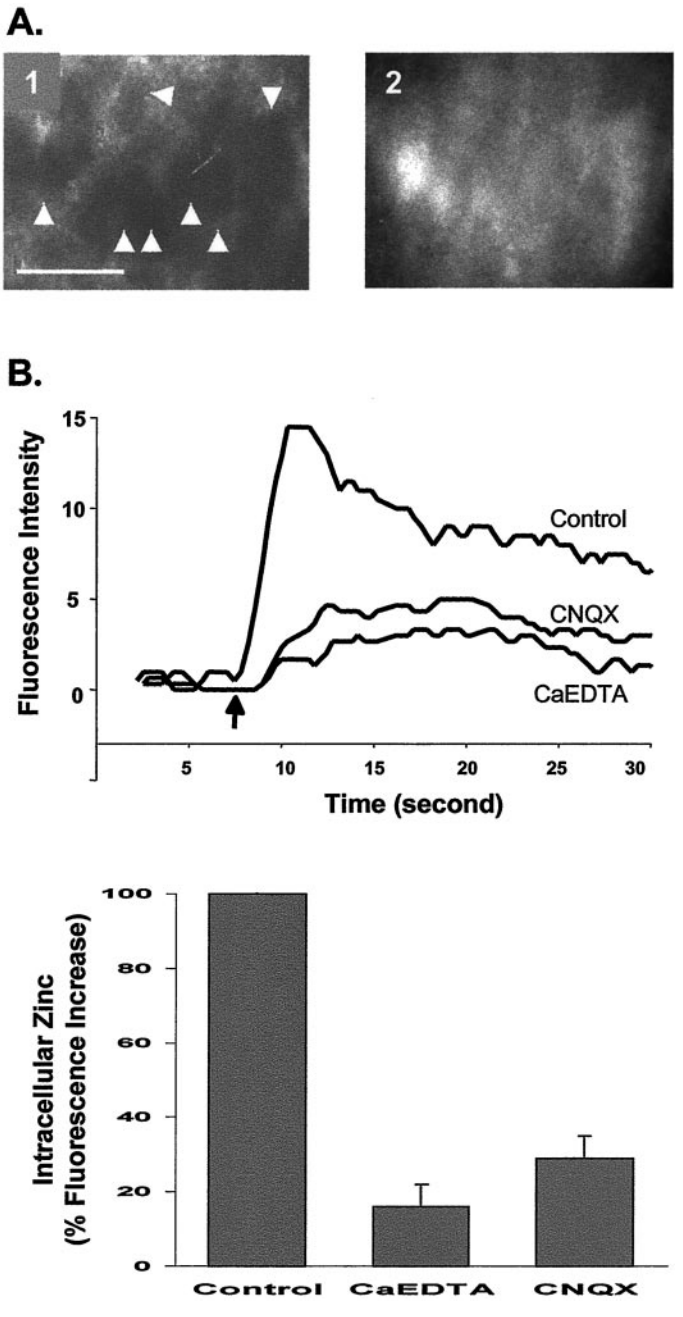

Figure 7. Increase of intracellular Zn^{2+} after HFS. *A*, Paired images of the pyramidal layer of CA3 taken with a 63× water immersion objective lens. Electrical stimulation increased intracellular Zn^{2+} in the CA3 region of hippocampal slices loaded with Newport Green diacetate (cell-permeable). Before stimulation (*1*), no cell bodies were labeled; they became visible (*2*) after stimulation (100 Hz, 500 μA for 10 sec). Scale bar, 50 μm; *arrowheads* indicate pyramidal cell bodies. *B*, Intracellular Zn^{2+} was detected with the fluorescence indicator Newport Green diacetate in normal ACSF and ACSF containing CaEDTA (10 mM) or CNQX (10 μM). The results are plotted on the *left*. the *arrow* indicates the beginning of stimulation. The *bar graph* on the *right* summarizes the effects of CaEDTA (n = 5) and CNQX (n = 3) on the increase in intracellular Zn^{2+} after electrical stimulation, expressed as percentage of control. Error bars indicate SEM.

rapid EPSP potentiation than did Zn^{2+} alone. These results indicate that glutamate enables the potentiating effect of Zn^{2+}.

Potentiation of the EPSP requires the entry of Zn^{2+} into neurons

One plausible explanation for this interaction is that glutamate is required to permit Zn^{2+} entry into pyramidal neurons. Glutamate allows Zn^{2+} to enter both directly through Ca^{2+}-permeable AMPA/kainate and NMDA receptors and indirectly, via its depolarizing effects, through VDCC (Choi and Koh, 1998; Weiss and Sensi, 2000). We directly tested whether glutamate mediates Zn^{2+} translocation across the postsynaptic membrane by the following experiments. Cells in the slice were loaded with Newport Green diacetate (the cell-permeable dye that, once inside the cell, is hydrolyzed by cytoplasmic esterases to become membrane-impermeable) and then thoroughly washed to eliminate unincorporated dye. Mossy fiber axons were then stimulated with HFS, and the entry of Zn^{2+} into cells in the CA3 pyramidal layer was imaged. In agreement with our previous findings, HFS caused an immediate influx of Zn^{2+} into cells (Fig. 7*A*). The

increase of intracellular Zn^{2+} fluorescence elicited by HFS was depressed by addition of either CaEDTA (10 mM) or CNQX (10 μM), an antagonist of AMPA/kainate receptors (Fig. 7*B*). The remaining fluorescence in the presence of 10 mM CaEDTA was likely caused by rapid entry of a small fraction of released Zn^{2+} into postsynaptic neurons or into presynaptic terminals. CNQX can block entry of Zn^{2+} not only through AMPA/kainate receptors but also through VDCC and NMDA receptors by preventing membrane depolarization by AMPA/kainate receptor channels. These results agree with our finding that CaEDTA blocks HFS-induced LTP by blocking Zn^{2+} entry into postsynaptic neurons.

Because CNQX blocked both Zn^{2+} translocation and LTP induction, we tested whether the introduction of Zn^{2+} into neurons by a different route could restore LTP. In several experiments, Zn^{2+} entry via ionotropic glutamate receptors and VDCC was blocked by 10 μM CNQX and 50 μM AP-5 (the NMDA receptor antagonist AP-5 was present in the perfusate throughout these experiments) but allowed to enter via sodium pyrithione, a selective Zn^{2+} ionophore (Zalewski et al., 1993), which directly increases intracellular Zn^{2+} (Fig. 8*A*). After washout of CNQX, Zn^{2+}, and Na-pyrithione, a long-lasting potentiation developed in the absence of HFS (158 ± 12%, mean ± SEM; n = 3). In contrast, without Na-pyrithione, addition of Zn^{2+} alone in the presence of CNQX failed to induce long-lasting potentiation of the EPSP (93 ± 9%, mean ± SEM; n = 4; Fig. 8*B*). Likewise, pyrithione (50 μM) alone, in the absence of Zn^{2+}, had no long-lasting effect on the EPSP (104 ± 5%, mean ± SEM; n = 5; data not shown). In slices loaded with intracellular Newport Green, which could also function as a selective intracellular Zn^{2+} chelator, the induction of LTP by HFS was blocked (110 ± 4.5%, mean ± SEM; Fig. 9). These data indicate that the translocation of extracellular Zn^{2+} into postsynaptic neurons is critical for the induction of LTP in mossy fiber→CA3 synapses and suggest an intracellular site of action for Zn^{2+}.

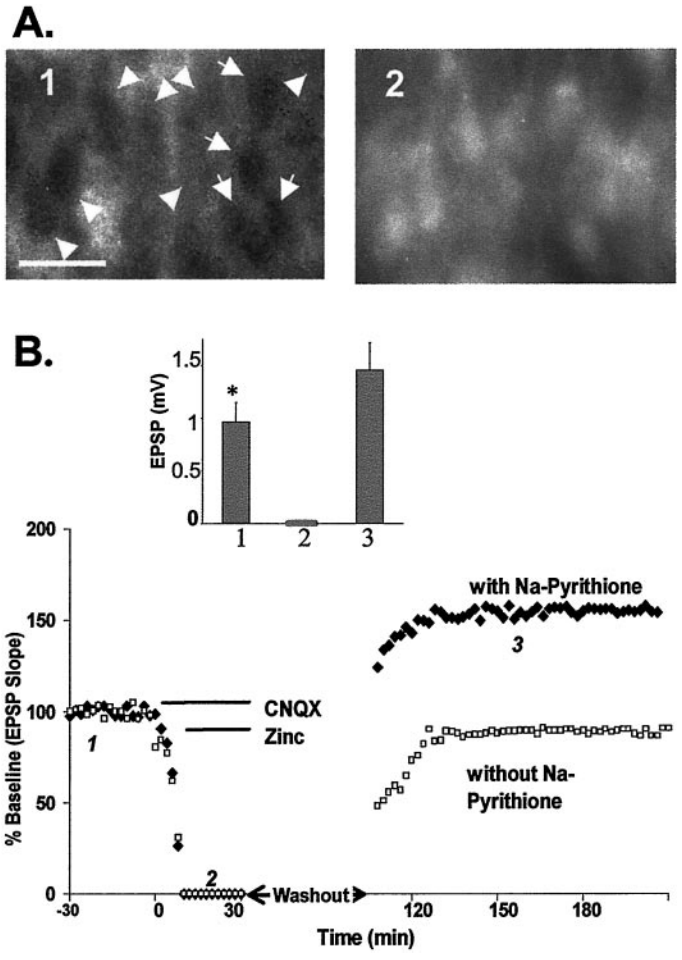

Figure 8. Potentiation of the EPSP requires entry of Zn^{2+} into cells. *A*, Paired images of the pyramidal layer of CA3 (taken with a 63× objective lens) loaded with Newport Green diacetate before (*1*) and after (*2*) exposure to Zn^{2+} (100 μM), Na-pyrithione (50 μM), and CNQX (10 μM). Scale bar, 50 μm; *arrowheads* indicate pyramidal cell bodies. *B*, Plot of the EPSP slope from a representative experiment to show that selectively increasing intracellular Zn^{2+} potentiates the EPSP (158 ± 12%; n = 4; *filled diamonds*). Zn^{2+} (100 μM) and Na-pyrithione (50 μM) were applied after the EPSP was blocked by CNQX (10 μM). In a similar experiment without Na-pyrithione, no EPSP potentiation was observed (93 ± 9%; n = 4; *open squares*). *Lines* indicate the duration of drug application. *Inset*, Summary of four experiments in which slices were treated with Na-pyrithione and Zn^{2+}. Values of the EPSP amplitude were taken from baseline (*1*), in the presence of CNQX (*2*), and during EPSP potentiation (*3*). *Numbers* correspond to those in *B*. *Significant difference ($p < 0.05$) between *1* and *3*.

DISCUSSION

Our results establish that synaptically released Zn^{2+} plays an essential role in the induction of LTP in mossy fiber→CA3 synapses. Effective Zn^{2+} chelation blocked the induction of LTP by HFS. Bath application of exogenous Zn^{2+} induced a long-lasting potentiation of the EPSP, apparently by acting at an intracellular site rather than at an extracellular site. Co-released glutamate is also essential for induction of LTP under physiological conditions, in part because it allows Zn^{2+} entry into postsynaptic neurons.

The mossy fiber→CA3 synapse contains high concentrations of Zn^{2+} in large synaptic boutons (Haug, 1967; Perez-Clausell and Danscher, 1985; Frederickson, 1989). This Zn^{2+} is released in the same manner as a neurotransmitter and is thought to be co-released with glutamate on stimulation of presynaptic terminals. We found that Zn^{2+} release is dependent on stimulation frequency (Li et al., 2001). Each mossy fiber bouton terminates on the proximal portion of apical CA3 dendrites with up to 35 release sites (Chicurel and Harris, 1992). Mossy fiber synapses show tremendous frequency facilitation that leads to plateau depolarizations during long stimulus trains (Vogt et al., 2000). Although we do not know the exact relationship between the prominent presence of Zn^{2+} and these unusual features, it indicates that these synapses are capable of rapidly releasing large amounts of Zn^{2+} during HFS. Therefore, it is not surprising that a high concentration of Zn^{2+} chelator was needed to buffer effectively the Zn^{2+} released during the HFS.

In this investigation of the possible role of Zn^{2+} in mossy fiber→CA3 synaptic plasticity, the removal of synaptically released Zn^{2+} with 10 mM CaEDTA blocked the induction of LTP. Direct fluorescence imaging showed that 10 mM CaEDTA chelated 85% of the synaptically released Zn^{2+}. This result verifies that the effect of CaEDTA on LTP induction in mossy fiber→CA3 synapses was achieved by its selective chelation of the synaptically released Zn^{2+} from mossy fiber terminals. On the other hand, a lower concentration of CaEDTA (1 mM) failed to reduce the extracellular Zn^{2+} after HFS, as evidenced by its inability to reduce Newport Green fluorescence. We have calculated that, under equilibrium conditions, 1 and 10 mM CaEDTA should indeed reduce 10–100 μM Zn^{2+} to 0.04–4 nM. The presence of 2.4 mM Ca^{2+} and 1.3 mM Mg^{2+} in the medium and

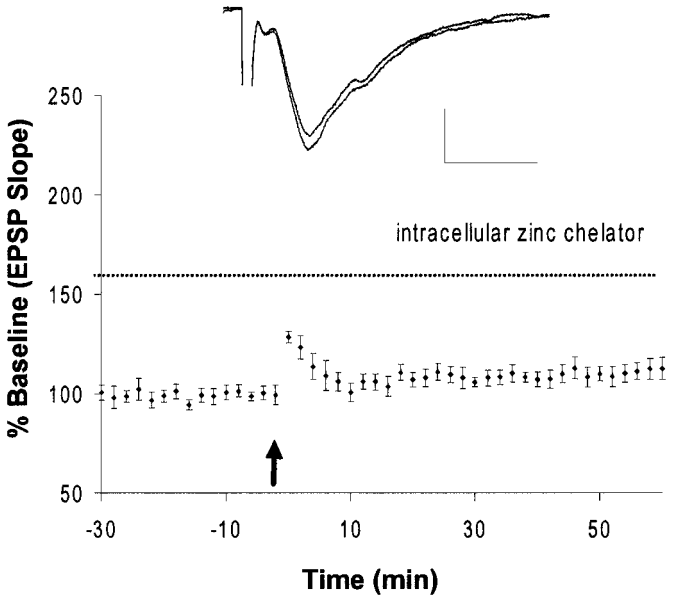

Figure 9. Intracellular Zn^{2+} chelator blocks the induction of LTP. HFS failed to induce mossy fiber LTP (110 ± 4.5%; $n = 4$) in slices loaded with intracellular Newport Green, which was used here as a selective intracellular Zn^{2+} chelator (*dashed line*). Each *point* represents the averaged and normalized EPSP initial negative slope, and error bars indicate SEM. *Inset*, EPSP recorded during baseline and at the end of recording after HFS. The *arrow* indicates HFS (100 Hz, 2 sec). Calibration: 1.0 mV, 5 msec.

the slow dissociation rate of CaEDTA, however, limit the rate at which Zn^{2+} is chelated (see Materials and Methods and Appendix). Kinetic calculations indicate that Zn^{2+} is chelated in a biphasic manner. The initial rate of chelation, limited by the initial concentration of free EDTA and rapidly dissociating MgEDTA, reaches completion in <0.1 msec. The slower phase, limited by the dissociation of CaEDTA, requires many seconds to reach completion at the equilibrium concentrations. Thus 1 mM CaEDTA was unable to prevent the micromolar accumulations of Zn^{2+} induced by HFS from mossy fiber terminals and entry into CA3 dendrites that we have observed to take place within milliseconds, because it provided a lower concentration of free EDTA and MgEDTA relative to the concentration of released Zn^{2+}. Ten millimolar CaEDTA, on the other hand, provided enough free EDTA and MgEDTA to reduce the 10–100 μM Zn^{2+} released by the mossy fiber terminals to concentrations below the level readily detected by Newport Green fluorescence as well as those required for LTP.

In the present study, the addition of 50–100 μM exogenous Zn^{2+} to the solution bathing the slice was required to induce a reliable, long-lasting potentiation of the EPSP. These data suggest that Zn^{2+} is able to enhance synaptic strength at mossy fiber→CA3 synapses. Ten micromolar Zn^{2+} did not appreciably alter synaptic transmission. Hence, it can be assumed that under stimulation conditions necessary to induce LTP, concentrations of >10 μM Zn^{2+} are released in the synapse. In addition, this may explain why the removal of Zn^{2+} released into the synaptic cleft during basal conditions or low-frequency stimulation failed to alter synaptic transmission. However, Zn^{2+} is able to inhibit the NMDA receptor at concentrations as low as 50 nM (Chen et al., 1997) and may play an important role in shaping the NMDA receptor response at this synapse under normal physiological conditions. Our results confirm the previous observation that, although a deficiency of bouton Zn^{2+} in rats resulted in the impairment of mossy fiber LTP, it does not appear to affect normal synaptic transmission (Lu et al., 2000). Thus, synaptically released Zn^{2+} appears to have little effect on basal synaptic function other than in modulating NMDA responses (Peters et al., 1987; Westbrook and Mayer, 1987; Chen et al., 1997) but is required for LTP induction by HFS in mossy fiber→CA3 synapses, which does not require NMDA receptor activation (Harris and Cotman, 1986). It is possible that Zn^{2+} may act on GABAergic interneurons resulting in an indirect effect on the pyramidal cell. Zn^{2+} inhibits hippocampal postsynaptic GABA current with a K_d of 11 μM (Mayer and Vyklicky, 1989). In our study, however, the removal of released Zn^{2+} or the addition of 10 μM exogenous Zn^{2+} did not alter synaptic transmission in mossy fiber→CA3 synapses. Furthermore, Zn^{2+} did not affect the afferent volley in our experimental conditions. We have therefore concluded that the indirect effects of Zn^{2+} acting on interneurons did not inhibit LTP at this synapse.

Because glutamate is also released from mossy fiber terminals during electrical stimulation, it is reasonable to expect that, under physiological conditions, both glutamate and Zn^{2+} are required for LTP induction in these terminals. The results from the present study indicate that glutamate promotes Zn^{2+} entry into the neuron by opening Zn^{2+}-permeable channels. It is known that glutamate allows Zn^{2+} to enter cultured neurons directly through Ca^{2+}-permeable AMPA/kainate and NMDA receptors and indirectly, via its depolarizing effects, through VDCC (Choi and Koh, 1998; Weiss and Sensi, 2000). In the present study, the increase of intracellular Zn^{2+} elicited by HFS was depressed by addition of CNQX, which can block entry of Zn^{2+} not only through AMPA/kainate receptors but also through VDCC and NMDA receptors by preventing membrane depolarization through the activation of AMPA/kainate receptors. We can rule NMDA receptors out, because we included APV in the ACSF. Toth et al. (2000) have reported that Ca^{2+}-permeable AMPA receptors are not expressed in CA3 principal neurons, raising doubt that these channels contribute significantly to Zn^{2+} entry in this region. Kainate receptors or VDCC remain as primary candidates. The possibility that these are the routes of Zn^{2+} entry in the proximal dendrites of CA3 pyramidal neurons in our experiments is also supported by the presence of a high density of VDCCs and putative Ca^{2+}-permeable kainate receptors in mossy fiber→CA3 synapses (Westenbroek et al., 1990; Bortolotto et al., 1999; Sui and Ruan, 2000). Ca^{2+} can enter the CA3 pyramidal neurons through these same channels. An increase in intracellular Ca^{2+} in postsynaptic neurons during LTP induction has been established for all hippocampal synapses except the mossy fiber→CA3 synapse (Zalutsky and Nicoll, 1990). Whether Ca^{2+} is required in the induction of mossy fiber LTP is the subject of many debates. Other groups have provided evidence that there is an initial rise in postsynaptic intracellular Ca^{2+} during LTP induction at the mossy fiber synapse (Yeckel et al., 1999). In these reports, LTP was prevented by chelation of postsynaptic intracellular Ca^{2+}. Interpretation of these results, however, is complicated by the fact that both the Ca^{2+} indicator and chelator used in those studies have higher affinities for Zn^{2+} than for Ca^{2+}. It is impossible to exclude in these studies the role of Zn^{2+} in LTP induction. A delineation of the separate roles of Zn^{2+} and Ca^{2+} in LTP induction and the possible interactions between these two ions will require further investigation.

One of the hallmarks of the mossy fiber synapse is its apparent lack of NMDA receptor-dependent synaptic plasticity. Some re-

Table 1. Kinetic constants used in calculating the Zn^{2+} concentration values in Figure 3

Ion	k_{on} (M/sec)	k_{off} (/sec)
Mg^{2+}	8.75×10^5	2.8
Ca^{2+}	2.20×10^7	0.7
Zn^{2+}	1×10^8	7×10^{-6}

ports have indicated that LTP at mossy fiber→CA3 synapses may be of presynaptic origin (Harris and Cotman, 1986; Nicoll and Malenka, 1999). However, in other studies, mossy fiber LTP has required both presynaptic and postsynaptic activation (Jaffe and Johnston, 1990). Many of these data could be explained by such factors as the type of LTP-inducing stimulus applied and the recording conditions, but the reasons for the conflicting results are still unclear. Although examining the presynaptic versus postsynaptic origin of LTP was not the goal of the present study, our results would support either a presynaptic or a postsynaptic origin of LTP. On release, Zn^{2+} could be taken up by selective high-affinity Zn^{2+} transporters in the mossy fiber terminals or could enter the postsynaptic neuron through glutamate and VDCC for induction of mossy fiber LTP. Our results cannot eliminate either mechanism for several reasons: First, CaEDTA prevented Zn^{2+} from entering both presynaptic terminals and postsynaptic neurons. Second, bath-applied Zn^{2+} could enter both mossy fiber terminals and CA3 neurons. Third, although CNQX blocked postsynaptic entry of Zn^{2+}, there may still be a substantial amount of Zn^{2+} taken up by presynaptic terminals, as indicated by the difference in the intracellular Newport Green fluorescence obtained in the presence of CaEDTA compared with that obtained with CNQX blockade after HFS. These arguments do not negate our observation, however, that Zn^{2+} must enter cells to perform its role in LTP induction through interactions with kinases, phosphatases, and other intracellular signaling pathways.

Our results introduce the idea that Zn^{2+} released from mossy fiber synapses acts as a presynaptically released second messenger or trans-synaptic factor. A presynaptically released factor that enhances synaptic strength could improve specificity and efficacy of synaptic transmission. In addition to its crucial role for gene expression and transcription, Zn^{2+} has been shown to activate a number of protein kinases such as protein kinase C (Hubbard et al., 1991; Quest et al., 1992), Ca/calmodulin kinase II (Brewer et al., 1979; Weinberger and Rostas, 1991; Lengyel et al., 2000), and mitogen-activated protein kinase (Park and Koh, 1999), which are associated with establishing LTP (Feng, 1995; Soderling and Derkach, 2000; Sweatt, 2001). Mossy fiber boutons terminate on the proximal portion of apical dendrites of CA3 pyramidal neurons. This unusual structure may give Zn^{2+} direct access to modulate gene transcription. Additionally, nanomolar Zn^{2+} signals modulate protein-tyrosine phosphatases and, thus, the phosphorylation of myriad postsynaptic proteins (Maret et al., 1999). Therefore, the present study raises the intriguing possibility that entry of synaptically released Zn^{2+} modulates intracellular signaling pathways and gene transcription.

APPENDIX

Calculations of Zn^{2+} chelation by CaEDTA in the presence of the ions in ACSF.

Our modeling of Zn^{2+} chelation by CaEDTA in the presence of the Ca^{2+} and Mg^{2+} in ACSF included both equilibrium and kinetics calculations. Although 1 mM CaEDTA may be adequate to remove released free Zn^{2+} by thermodynamic arguments, the kinetics of chelation may be too slow to achieve adequate removal within the time frame of a synaptic event. Equilibrium constants were obtained from Martell and Smith (1974) and Bers et al. (1994). Kinetic constants were obtained from Davis et al. (1999) and Hering and Morel (1988) (Table 1). In the absence of an experimentally derived on-rate for Zn^{2+} complexing with EDTA, we used the rate of diffusion (10^8 M/sec) as the rate that limits Zn^{2+}–EDTA complex formation. The off-rate constant was then calculated from the K_d. The equations used for the equilibrium case are as follows:

Let C, M, Z, and E represent the concentrations of the free ions of calcium, magnesium, zinc, and EDTA, respectively. CE, ME, and ZE represent the concentrations of the EDTA complexes of Ca^{2+}, Mg^{2+}, and Zn^{2+}, respectively. C_T, M_T, Z_T, and E_T represent the total concentrations of Ca^{2+}, Mg^{2+}, Zn^{2+}, and EDTA, respectively. K_C, K_M, and K_Z represent the equilibrium dissociation constants for Ca^{2+}, Mg^{2+}, and Zn^{2+}, respectively. Total concentration of any one metal ion is the sum of chelated and free ions. Thus:

$$CE = C_T - C, \quad ME = M_T - M, \quad ZE = Z_T - Z. \tag{1}$$

Total EDTA in solution is given by:

$$E_T = E + CE + ME + ZE. \tag{2}$$

Substituting the chelated forms for the expressions containing total concentrations in Equation 1 and rearranging, the total concentrations on the left:

$$E_T - C_T - M_T - Z_T = E - C - M - Z. \tag{3}$$

$$K_T = E_T - C_T - M_T - Z_T. \quad \text{Then, } K_T = E - C - M - Z. \tag{4}$$

Table 2. Equilibrium constants and Zn^{2+} concentration in ACSF at two different concentrations of total Zn^{2+} and CaEDTA

$[Zn^{2+}]_T$ (μM)	$[CaEDTA]_T$ (mM)	$[Zn^{2+}]$ (M)	$K_{Zn^{2+}}$ (M)	$K_{Ca^{2+}}$ (M)	$K_{Mg^{2+}}$ (M)
100	10	3.68×10^{-11}	4.16×10^{-14}	3.01×10^{-8}	1.20×10^{-6}
	1	3.55×10^{-9}	4.00×10^{-14}	2.9×10^{-8}	1.1×10^{-6}
10	10	3.53×10^{-11}	4.16×0^{-14}	3.01×10^{-8}	1.20×10^{-6}
	1	3.21×10^{-10}	4.00×10^{-14}	2.90×10^{-8}	1.10×10^{-6}

At 32°C, pH 7.4, ionic strength 0.159.

Rearranging the definition of the dissociation constants and substituting Equation 1 for the chelated forms:

$$E = K_C \cdot (C_T - C)/C, \quad E = K_M \cdot (M_T - M)/M,$$

$$E = K_Z \cdot (Z_T - Z)/Z, \quad (5)$$

we can derive three equations by substituting Equation 5 in Equation 4:

$$K_T = (K_C \cdot (C_T - C)/C) - C - M - Z, \quad (6)$$

$$K_T = (K_M \cdot (M_T - M)/M) - C - M - Z, \quad (7)$$

$$K_T = (K_Z \cdot (Z_T - Z)/Z) - C - M - Z. \quad (8)$$

Equations 6–8 are quadratic equations, each with three unknowns. They could be solved simultaneously, but we used an iterative calculation method using Microsoft Excel. Estimates were made of each ion concentration initially in the absence of Zn^{2+} and then including Zn^{2+}, and a calculated value was determined using Equations 6–8, in order of increasing affinity for EDTA. With each calculation, the calculated value was substituted for the estimate made for that ion. A macro was created to do this iteratively until the difference between the calculated and estimated values for Mg^{2+} concentration was less than an arbitrary critical value (1×10^{-9}). The results for Zn^{2+} concentration are shown in Table 2. The equilibrium values for Ca^{2+}, Mg^{2+}, and Zn^{2+} agreed with those calculated by WEBMAXC version 2.10 (www.stanford.edu/~cpatton/webmaxc2.htm) using the same equilibrium constants (Table 2). Our estimates of equilibrium concentrations assumed a temperature of 32°C, pH 7.40, and an ionic strength of 0.159 for ACSF.

The kinetics of Zn^{2+} chelation were calculated as follows: Let k_{off} and k_{on} be the dissociation and association rate constants. Then:

$$dZ/dt = k_{on} \cdot Z \cdot E - k_{of} \cdot ZE = k_{on} \cdot Z \cdot E - k_{of} \cdot (Z_T - Z). \quad (9)$$

Substituting Equation 4 for E in Equation 9, the rate of zinc chelation can be calculated from the concentrations of the three metal ions and other constants:

$$dZ/dt = k_{on} \cdot Z \cdot (K_T + C + M + Z) - k_{of} \cdot (Z_T - Z). \quad (10)$$

This equation is also quadratic. The equations for the other ions were derived in the same way and have the same form. Again, we used an Excel spreadsheet to calculate an approximation of the concentrations of each of the three metal ions over time from initial conditions using an appropriately small interval (1×10^{-7} sec). The initial conditions chosen were consistent with our experimental conditions. These take the concentrations of Ca^{2+} and Mg^{2+} in ACSF to be those at equilibrium with the given concentration of CaEDTA in the absence of Zn^{2+}. The given concentration of Zn^{2+} was assumed to be released instantaneously into the medium at time 0. Figure 3 shows the time course of Zn^{2+} concentration change over the course of 0.1 msec, a time frame considered typical for neurotransmitter release.

REFERENCES

Aniksztejn L, Charton G, Ben-Ari Y (1987) Selective release of endogenous zinc from the hippocampal mossy fibers in situ. Brain Res 404:58–64.

Assaf SY, Chung SH (1984) Release of endogenous Zn2+ from brain tissue during activity. Nature 308:734–736.

Basolo F, Pearson RG (1967) Mechanisms of inorganic reactions; a study of metal complexes in solution, Ed 2. New York: Wiley.

Bers DM, Patton CW, Nuccitelli R (1994) A practical guide to the preparation of Ca^{2+} buffers. Methods Cell Biol 40:3–29.

Bortolotto ZA, Clarke VR, Delany CM, Parry MC, Smolders I, Vignes M, Ho KH, Miu P, Brinton BT, Fantaske R, Ogden A, Gates M, Ornstein PL, Lodge D, Bleakman D, Collingridge GL (1999) Kainate receptors are involved in synaptic plasticity. Nature 402:297–301.

Bramham CR, Sarvey JM (1996) Endogenous activation of mu and delta-1 opioid receptors is required for long-term potentiation induction in the lateral perforant path: dependence on GABAergic inhibition. J Neurosci 16:8123–8131.

Brewer GJ, Aster JC, Knutsen CA, Kruckeberg WC (1979) Zinc inhibition of calmodulin: a proposed molecular mechanism of zinc action on cellular functions. Am J Hematol 7:53–60.

Chen N, Moshaver A, Raymond LA (1997) Differential sensitivity of recombinant *N*-methyl-D-aspartate receptor subtypes to zinc inhibition. Mol Pharmacol 51:1015–1023.

Chicurel ME, Harris KM (1992) Three-dimensional analysis of the structure and composition of CA3 branched dendritic spines and their synaptic relationships with mossy fiber boutons in the rat hippocampus. J Comp Neurol 325:169–182.

Choi DW, Koh JY (1998) Zinc and brain injury. Annu Rev Neurosci 21:347–375.

Davis JP, Tikunova SB, Walsh MP, Johnson JD (1999) Characterizing the response of calcium signal transducers to generated calcium transients. Biochemistry 38:4235–4244.

Dawson RMC, Elliot DC, Elliot WH, Jones KM (1986) Data for biochemical research, Ed 3. New York: Oxford.

Feng TP (1995) The involvement of PKC and multifunctional CaM kinase II of the postsynaptic neuron in induction and maintenance of long-term potentiation. Prog Brain Res 105:55–63.

Fredens K, Danscher G (1973) The effect of intravital chelation with dimercaprol, calcium disodium edetate, 1–10-phenantroline and 2,2′-dipyridyl on the sulfide silver stainability of the rat brain. Histochemie 37:321–331.

Frederickson CJ (1989) Neurobiology of zinc and zinc-containing neurons. Int Rev Neurobiol 31:145–238.

Frederickson CJ, Suh SW, Silva D, Thompson RB (2000) Importance of zinc in the central nervous system: the zinc-containing neuron. J Nutr 130:1471.S–1483.S.

Golub MS, Keen CL, Gershwin ME, Hendrickx AG (1995) Developmental zinc deficiency and behavior. J Nutr 125:2263.S–2271.S.

Harris EW, Cotman CW (1986) Long-term potentiation of guinea pig mossy fiber responses is not blocked by *N*-methyl-D-aspartate antagonists. Neurosci Lett 70:132–137.

Haug FM (1967) Electron microscopical localization of the zinc in hippocampal mossy fibre synapses by a modified sulfide silver procedure. Histochemie 8:355–368.

Hering JG, Morel FMM (1988) Kinetics of trace metal complexation: role of alkaline-earth metals. Environ Sci Technol 22:1469–1478.

Howell GA, Welch MG, Frederickson CJ (1984) Stimulation-induced uptake and release of zinc in hippocampal slices. Nature 308:736–738.

Hubbard SR, Bishop WR, Kirschmeier P, George SJ, Cramer SP, Hendrickson WA (1991) Identification and characterization of zinc binding sites in protein kinase C. Science 254:1776–1779.

Jaffe D, Johnston D (1990) Induction of long-term potentiation at hippocampal mossy-fiber synapses follows a Hebbian rule. J Neurophysiol 64:948–960.

Kamiya H, Shinozaki H, Yamamoto C (1996) Activation of metabotropic glutamate receptor type 2/3 suppresses transmission at rat hippocampal mossy fibre synapses. J Physiol (Lond) 493:447–455.

Lengyel I, Fieuw-Makaroff S, Hall AL, Sim AT, Rostas JA, Dunkley PR (2000) Modulation of the phosphorylation and activity of calcium/calmodulin-dependent protein kinase II by zinc. J Neurochem 75:594–605.

Li Y, Hough CJ, Suh SW, Sarvey JM, Frederickson CJ (2001) Rapid Translocation of Zn^{2+} from presynaptic terminals into postsynaptic hippocampal neurons following physiological stimulation. J Neurophysiol, in press.

Lu Y, Taverna FA, Tu R, Ackerley CA, Wang Y-T, Roder J (2000) Endogenous Zn^{2+} is required for the induction of long-term potentiation (LTP) at rat hippocampal mossy fiber-CA3 synapses. Synapse 38:187–197.

Maret W, Jacob C, Vallee BL, Fischer EH (1999) Inhibitory sites in enzymes: zinc removal and reactivation by thionein. Proc Natl Acad Sci USA 96:1936–1940.

Martell AE, Smith RM (1974) Critical stability constants. New York: Plenum.

Mayer ML, Vyklicky Jr L (1989) The action of zinc on synaptic transmission and neuronal excitability in cultures of mouse hippocampus. J Physiol (Lond) 415:351–365.

Nicoll RA, Malenka RC (1999) Expression mechanisms underlying NMDA receptor-dependent long-term potentiation. Ann NY Acad Sci 868:515–525.

Palmiter RD, Cole TB, Quaife CJ, Findley SD (1996) ZnT-3, a putative

transporter of zinc into synaptic vesicles. Proc Natl Acad Sci USA 93:14934–14939.
Park JA, Koh JY (1999) Induction of an immediate early gene egr-1 by zinc through extracellular signal-regulated kinase activation in cortical culture: its role in zinc-induced neuronal death. J Neurochem 73:450–456.
Perez-Clausell J, Danscher G (1985) Intravesicular localization of zinc in rat telencephalic boutons. A histochemical study. Brain Res 337:91–98.
Peters S, Koh J, Choi DW (1987) Zinc selectively blocks the action of *N*-methyl-D-aspartate on cortical neurons. Science 236:589–593.
Quest AF, Bloomenthal J, Bardes ES, Bell RM (1992) The regulatory domain of protein kinase C coordinates four atoms of zinc. J Biol Chem 267:10193–10197.
Soderling TR, Derkach VA (2000) Postsynaptic protein phosphorylation and LTP. Trends Neurosci 23:75–80.
Sui L, Ruan DY (2000) Impairment of the Ca2+-permeable AMPA/kainate receptors by lead exposure in organotypic rat hippocampal slice cultures. Pharmacol Toxicol 87:204–210.
Sweatt JD (2001) The neuronal MAP kinase cascade: a biochemical signal integration system subserving synaptic plasticity and memory. J Neurochem 76:1–10.
Toth K, Suares G, Lawrence JJ, Philips-Tansey E, McBain CJ (2000) Differential mechanisms of transmission at three types of mossy fiber synapse. J Neurosci 20:8279–8289.
Vogt K, Mellor J, Tong G, Nicoll R (2000) The actions of synaptically released zinc at hippocampal mossy fiber synapses. Neuron 26:187–196.
Weinberger RP, Rostas JA (1991) Effect of zinc on calmodulin-stimulated protein kinase II and protein phosphorylation in rat cerebral cortex. J Neurochem 57:605–614.
Weiss JH, Sensi SL (2000) Ca2+-Zn2+ permeable AMPA or kainate receptors: possible key factors in selective neurodegeneration. Trends Neurosci 23:365–371.
Weiss JH, Koh JY, Christine CW, Choi DW (1989) Zinc and LTP [letter]. Nature 338:212.
Westbrook GL, Mayer ML (1987) Micromolar concentrations of Zn2+ antagonize NMDA and GABA responses of hippocampal neurons. Nature 328:640–643.
Westenbroek RE, Ahlijanian MK, Catterall WA (1990) Clustering of L-type Ca2+ channels at the base of major dendrites in hippocampal pyramidal neurons. Nature 347:281–284.
Yeckel MF, Kapur A, Johnston D (1999) Multiple forms of LTP in hippocampal CA3 neurons use a common postsynaptic mechanism. Nat Neurosci 2:625–633.
Zalewski PD, Forbes IJ, Betts WH (1993) Correlation of apoptosis with change in intracellular labile Zn(II) using zinquin [(2-methyl-8-*p*-toluenesulphonamido-6-quinolyloxy)acetic acid], a new specific fluorescent probe for Zn(II). Biochem J 296:403–408.
Zalutsky RA, Nicoll RA (1990) Comparison of two forms of long-term potentiation in single hippocampal neurons. Science 248:1619–1624.